Letter to the Editor

The contribution of T2 relaxation time to MRI-derived apparent diffusion coefficient (ADC) quantification and its potential clinical implications

Yì Xiáng J. Wáng[1], Kai-Xuan Zhao[2], Fu-Zhao Ma[1], Ben-Heng Xiao[1]

[1]Department of Imaging and Interventional Radiology, Faculty of Medicine, The Chinese University of Hong Kong, Hong Kong, China; [2]Department of Radiology, Guangdong Provincial People's Hospital, Guangdong Academy of Medical Sciences, Southern Medical University, Guangzhou, China

Correspondence to: Yì Xiáng J. Wáng, MMed, PhD. Department of Imaging and Interventional Radiology, Faculty of Medicine, The Chinese University of Hong Kong, 30-32 Ngan Shing Street, Shatin, New Territories, Hong Kong, China. Email: yixiang_wang@cuhk.edu.hk.

Submitted Aug 03, 2023. Accepted for publication Aug 29, 2023. Published online Sep 06, 2023.
doi: 10.21037/qims-23-1106
View this article at: https://dx.doi.org/10.21037/qims-23-1106

Intravoxel incoherent motion (IVIM) theory in magnetic resonance imaging (MRI) was proposed by Le Bihan *et al.* to account for the effect of vessel/capillary perfusion on the aggregate diffusion weighted MR signal. The fast component of diffusion is related to perfusion, whereas the slow component is linked to tissue molecular diffusion. The prevalent IVIM modeling is based on Eq. [1]:

$$SI_{(b)}/SI_{(0)} = (1-PF)\times\exp(-b\times D_{slow}) + PF\times\exp(-b\times D_{fast}) \quad [1]$$

where $SI_{(b)}$ and $SI_{(0)}$ denote the signal intensity of images acquired with the *b*-factor value of *b* and *b*=0 s/mm^2, respectively. Three parameters can be computed. D_{slow} (or *D*) is the diffusion coefficient representing the slow molecular diffusion only minimally affected by perfusion. The perfusion fraction (*PF*, or *f*) represents the fraction of the compartment related to circulation, which can be understood as the proportional 'incoherently flowing fluid' (i.e., blood) volume. D_{fast} (or *D**) is the perfusion-related diffusion coefficient which holds information for blood perfusion's speed. Recently, we demonstrated that, using liver as the reference, IVIM derived *PF* for the spleen is underestimated approximately by half (1). Literature also consistently reports a lower spleen D_{slow} than liver D_{slow} (1). With our own data (n=20 healthy volunteers), liver D_{slow} was estimated to be 1.06±0.10 (×10^{-3} mm^2/s) and spleen D_{slow} was 0.89±0.17. Since D_{slow} has a limited dynamic range (2), this difference of 0.17 (×10^{-3} mm^2/s) between liver D_{slow} and spleen D_{slow} can be considered substantial [this is also consistent with other reports (2)].

Hereby, we argue that spleen D_{slow} is also substantially underestimated by IVIM if we consider liver D_{slow} as the reference. Since the liver and spleen have similar vessel volume and blood flow per tissue volume per minute, and the spleen is waterier than the liver (T1/T2 relaxation is 1,328/61 ms for spleen and 809/34 ms for liver at 3.0 T, *Figure 1*) (2,3), it is quite unlikely that spleen D_{slow} is much lower than liver D_{slow}. While there is no other reference measure for water diffusion *in vivo*, the magnetization transfer signal ratio (MTR) measure shows a higher proportion of water molecules in the liver are bound to other macro-molecules than the water molecules in the spleen (4), which supports that water molecules in the spleen have a greater extent of free diffusion. Free water molecules also allow longer T1 and T2 relaxation times than bounded water molecules. The spleen is also an organ with the function of storing blood (5). The spleen can respond to sympathetic stimulation by contracting its fibroelastic capsule and trabeculae to increase systemic blood supply. Another point of consideration is that liver has higher iron content and shorter T2* relaxation time than the spleen (3,6), and it has been well noted that iron content and shorter T2* relaxation time are associated with lower measured apparent diffusion coefficient (ADC) or D_{slow} (7,8). Despite all these, the fact that measured spleen D_{slow} is much lower than liver D_{slow} strongly suggests

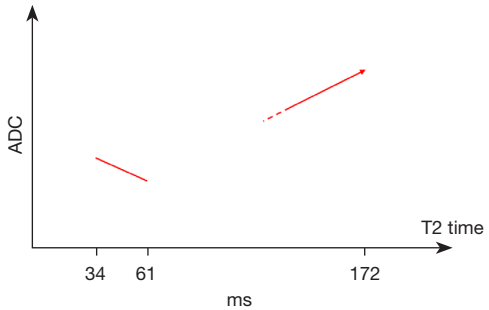

Figure 1 Hypothesized relationship between tissue ADC and tissue T2 relaxation time *in vivo*. Around the tissue T2 relaxation time of 34 ms (liver tissue at 3T) and 61 ms (spleen tissue at 3T), a negative relationship exists between ADC value and tissue T2 relaxation time. However, around and till the T2 relaxation time for gallbladder (172 ms at 3T), a positive relationship exists between ADC value and T2 relaxation time. ADC, apparent diffusion coefficient.

spleen D_{slow} is underestimated by IVIM. It has been well noted that the spleen ADC is also much lower than the liver ADC (9). Considering liver as the reference, that both fast diffusion (*PF*) and slow diffusion (D_{slow}) of the spleen are much underestimated is likely due to the MRI properties of the spleen such as the much longer T2 relaxation time. The well noted 'T2 shine-through' phenomenon demonstrates the effect of T2 relaxation time on diffusion weighted image signal. It is possible that, around the range of T2 time of spleen, longer T2 relaxation time leads to lower diffusion measure (*Figure 1*). This phenomenon will not be limited to the spleen, thus we shall keep this in mind when we consider all MRI measured diffusion effects including ADC. More examples are given in *Table 1* for myometrium tumors [myometrium's T2 is 79 ms at 3T (3)].

Table 1 shows, when the uterine myometrium tumors

Table 1 Relationship between myometrium tumor T2 weighted signal intensity and tumor diffusion restriction

Tissue type [scenario number]	Diffusion on ADC map			Signal on T2 weighted images
	Restricted	Unknown	Not restricted	
DeMulder *et al.* LM cystic degenerated [1]	–	–	Yes	H-hyperintense
DeMulder *et al.* LM myxoid degenerated [2]	–	–	Yes	H-hyperintense
Barral *et al.* Cellular LM [3]	Yes	–	–	Hyperintense
DeMulder *et al.* Cellular LM [4]	Yes	–	–	Hyperintense
Bura *et al.* Highly cellular LM [5]	Yes	–	–	Hyperintense
Bura *et al.* Leiomyosarcoma [6]	Yes	–	–	Hyperintense
Barral *et al.* Leiomyosarcoma [7]	Yes	–	–	Hyperintense
Barral *et al.* Common LM [8]	–	–	Yes	Hypointense
Bura *et al.* Ordinary LM [9]	–	–	Yes	Hypointense
DeMulder *et al.* LM hyaline degenerated [10]	–	–	Yes	Hypointense
DeMulder *et al.* LM carneous degenerated [11]	–	–	Yes	Hypointense
DeMulder *et al.* LM-calcific degenerated [12]	–	–	Yes	Hypointense
DeMulder *et al.* Lipoleiomyoma [13]	–	Yes	–	Heterogeneous
DeMulder *et al.* STUMP [14]	–	Yes	–	Heterogeneous
Barral *et al.* Degenerated LM [15]	–	–	Yes	Heterogeneous

Summarized from *Tab. 2* by DeMulder *et al.* (10), *Tab. 1* by Bura *et al.* (11), and *Tab. 1* by Barral *et al.* (12). ADC, apparent diffusion coefficient; LM, leiomyoma; H-hyperintense, highly hyperintense; STUMP, smooth muscle tumors of uncertain malignant potential.

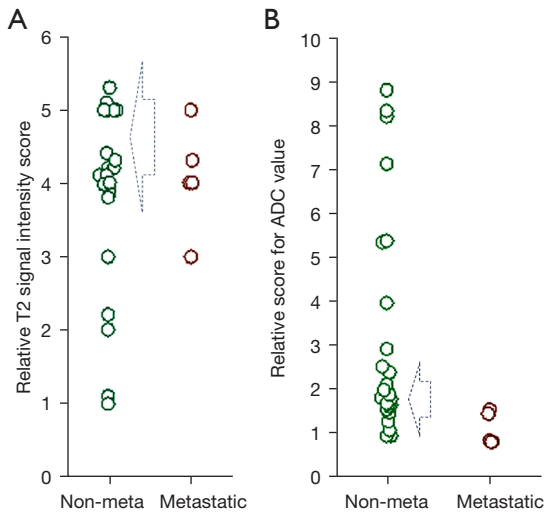

Figure 2 Possible negative relationship between ADC value and T2 relaxation time for renal carcinoma. The Y-axis in (A) denotes relative score for T2 relaxation time, with higher score associated with longer T2 relaxation time. The Y-axis in (B) denotes relative score for ADC, with higher score associated with higher ADC value. Arrow denotes the non-metastatic (non-meta, green circles) tumors with longer T2 relaxation time tend to have lower ADC value. Metastatic tumors (red circles) are associated with low ADC value and long T2 relaxation time. Data are re-drawn from Paudyal *et al.* (13). ADC, apparent diffusion coefficient.

are T2 weighted signal intensity hypertensive (i.e., longer T2 time relative to myometrium), these tumors likely show diffusion restriction (scenarios 3–7). This is similar to that, while the spleen is signal intensity hypertensive relative to the liver, spleen demonstrates diffusion restriction relative to the liver. On the other hand, when the tumors are T2 weighted signal intensity hypotensive (i.e., shorter T2 time relative to uterine myometrium), these tumors likely show no diffusion restriction (scenarios 8–12). When the tumors have heterogeneous T2 weighted signal, they were noted as without diffusion restriction or diffusion restriction unknown. However, when the lesions are very highly hyperintense such as the cases of leiomyoma cystic degeneration and myxoid degeneration (scenarios 1–2), the relation between T2 weighted signal intensity and diffusion is similar to that of a normal gallbladder, i.e., T2 weighted signal intensity highly hyperintense without diffusion restriction (*Figure 1*). For renal carcinoma, a possible negative correlation between ADC value and T2 value can be noted (*Figure 2*).

Hereby we discuss two possible implications with high clinical relevance. Most liver tumors have a longer T2 relaxation time than their native normal tissue and this is considered to be associated with oedema. On the other hand, most tumors are measured with lower MRI diffusion (despite being oedematous) (14). The reason why malignant tumors have lower diffusion value (ADC and D_{slow}) is poorly understood but has been proposed to be related to a combination of higher cellularity, tissue disorganization, and increased extracellular space tortuosity (14). These explanations may be true, but it is also possible that many tumors have MRI properties similar to the spleen such as longer T2 (relative to the liver) and these MRI properties may also contribute to the lower MRI measured ADC and D_{slow} (*Figures 3*,*4*). In other words, if we could hypothetically plant a piece of spleen tissue in the liver, MRI would recognize this planted spleen tissue as being similar to a tumor and measure it to have lower diffusion than the liver. Actually, a case report of intrahepatic splenosis, with the presence of acquired ectopic splenic tissue with a history of splenectomy after splenic rupture from trauma, has been reported (16). Intrahepatic splenosis was noted to show high signal on T2 weighted and diffusion weighted images with corresponding very low signals on ADC images. Note that, Nonomura *et al.* (17) reported there was no ADC difference between normal hematopoietic cell bone marrow without fat infiltration and lymphoma-related hypercellular bone marrow, despite lymphoma tissue had more compacted cells. Following the example of spleen tissue, *PF* of liver tumors could be underestimated by IVIM as well. Another possible implication will be the interpretation of diffusion measures after brain ischemia. After cerebral artery occlusion, diffusion decreases in the very acute phase while T2 relaxation time remains unchanged. After that, T2 relaxation time starts to increase, then diffusion starts to rise to the baseline level and then further rises to a higher level (18,19) (*Figure 5*). If a longer T2 relaxation time 'depresses' MRI diffusion measure, at some point, such as 24 hours after the occlusion when the T2 relaxation time is already very elongated (*Figure 5*), the diffusion in the ischemic area could be highly underestimated by MRI. Note, some brain regions have T2 relaxation similar to that of spleen (20). However, there is a limit on how longer T2 relaxation time can 'depress' MRI diffusion measure (*Figure 1*). For example, the gallbladder measures high diffusion value (D_{slow} and ADC of around 3.0×10^{-3} mm^2/s for our

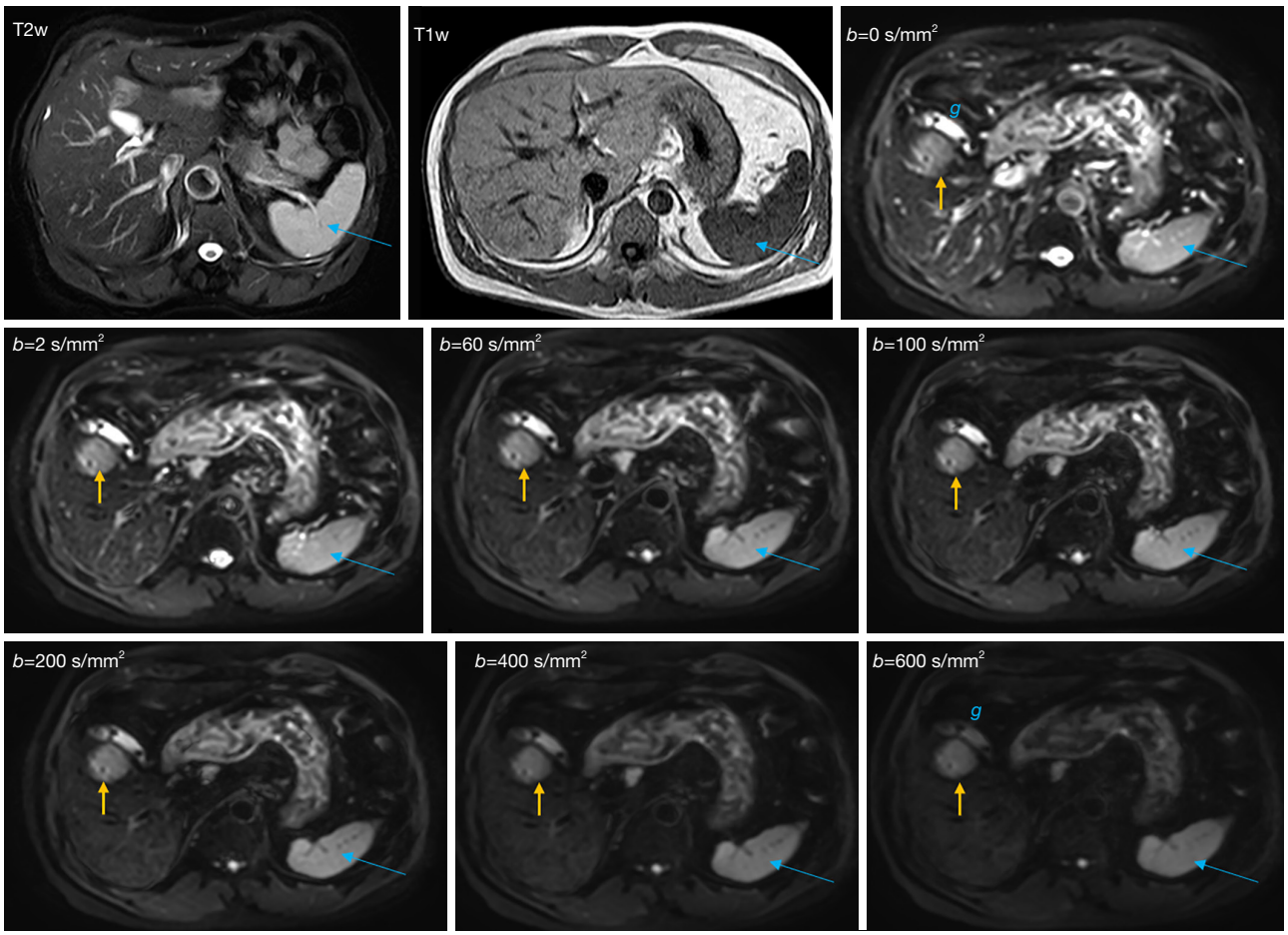

Figure 3 T2w, T1w, and diffusion weighted (b=0–600 s/mm^2) MR images of liver and spleen. T2w and T1w images are from two volunteers without liver or spleen lesions. Compared the liver, the spleen (blue arrow) shows higher signal on T2w image and lower signal on T1w image, consistent with that spleen has longer T1/longer T2 property and appears to be waterier. Diffusion weighted images are from a hepatocarcinoma patient with liver fibrosis caused by type-b viral hepatitis. It appears that the tumor (orange arrow) and the spleen show a similar signal decay trend following the increasing b-values. Both the tumor and the spleen show higher signal than the liver on all diffusion weighted images. g, gallbladder; T2w, T2-weighted; T1w, T1-weighted; MR, magnetic resonance.

in vivo measure). *Table 1* also shows, when T2 is very long such as those of the leiomyoma cystic degeneration and myxoid degeneration, the ADC values might be high. Note that, the influence of T2 on IVIM parameter estimation has already been demonstrated and extended IVIMs models including T2 relaxation times have been proposed (21,22). However, it appears that that the application these extended IVIMs models mainly change the IVIM-*PF* measure, but not the IVIM-D_{slow} measure. Since nearly all tissues are dominated by slow diffusion with only a smaller contribution by fast diffusion, current diffusion models considering T2 time may not solve the problem for ADC satisfactorily discussed in this letter. Therefore, our arguments suggest new venues for future studies and validation for MRI derived diffusion parameters such as ADC (even though it has already been widely applied clinically).

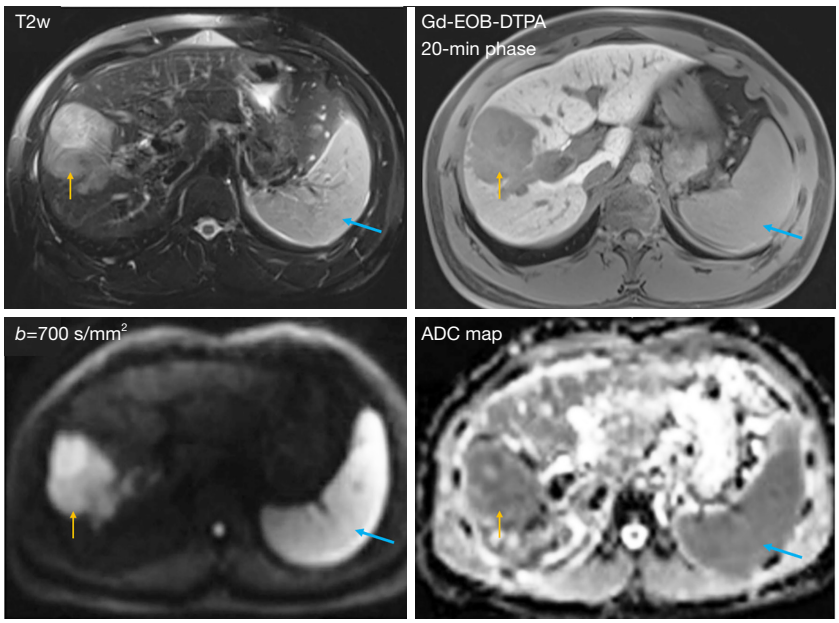

Figure 4 T2w, T1-weighted Gd-EOB-DTPA enhanced 20-minute hepatobiliary phase, diffusion weighted (b=700 s/mm^2) MR images, and ADC map of the liver, a hepatocellular carcinoma (orange arrow) and the spleen (blue arrow). Though the tumor has heterogeneous structures, it appears that the tumor and the spleen show many signal similarities on these four images. The lower spleen ADC value than the liver ADC value is likely due to a quantification error as described in this letter. Reproduced from Cao *at al*. (15). T2w, T2-weighted; ADC, apparent diffusion coefficient; Gd-EOB-DTPA, gadolinium ethoxybenzyl diethylenetriamine pentaacetic acid; MR, magnetic resonance.

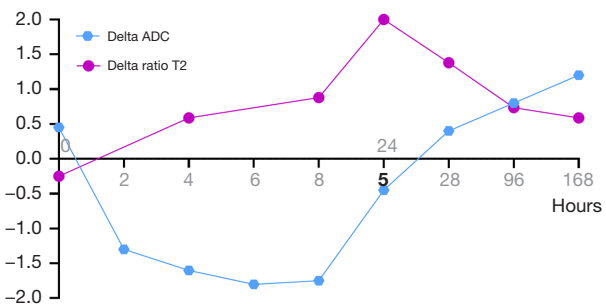

Figure 5 A schematic presentation of the time course changes of ADC and T2 relaxation time in the ischemic region after a cerebral artery occlusion. The data are approximated from the rat experimental study of Knight *et al*. (19). ADC (10^{-3} mm^2/s) is presented as values changed from normal tissue measure. T2 relaxation time is presented relatively in ratio with an increase of 46 milliseconds as a value of 2 in the graph. X-axis: hours after cerebral artery occlusion. ADC, apparent diffusion coefficient.

Acknowledgments

Some results of this letter have been posted on preprint arXiv:2306.10657 and arXiv:2306.02011.

Funding: This work was supported by Hong Kong GRF Projects (Nos. 14109218 and 14112521).

Footnote

Provenance and Peer Review: This article was a standard submission to the journal. The article has undergone external peer review.

Conflicts of Interest: All authors have completed the ICMJE uniform disclosure form (available at https://qims.amegroups.com/article/view/10.21037/qims-23-1106/coif). YXJW serves as the Editor-in-Chief of *Quantitative Imaging*

in Medicine and Surgery. The other authors have no conflicts of interest to declare.

Ethical Statement: The authors are accountable for all aspects of the work in ensuring that questions related to the accuracy or integrity of any part of the work are appropriately investigated and resolved.

References

1. Yu WL, Xiao BH, Ma FZ, Zheng CJ, Tang SN, Wáng YXJ. Underestimation of the spleen perfusion fraction by intravoxel incoherent motion MRI. NMR Biomed 2023;36:e4987.
2. Li YT, Cercueil JP, Yuan J, Chen W, Loffroy R, Wáng YX. Liver intravoxel incoherent motion (IVIM) magnetic resonance imaging: a comprehensive review of published data on normal values and applications for fibrosis and tumor evaluation. Quant Imaging Med Surg 2017;7:59-78.
3. de Bazelaire CM, Duhamel GD, Rofsky NM, Alsop DC. MR imaging relaxation times of abdominal and pelvic tissues measured in vivo at 3.0 T: preliminary results. Radiology 2004;230:652-9.
4. Martirosian P, Boss A, Deimling M, Kiefer B, Schraml C, Schwenzer NF, Claussen CD, Schick F. Systematic variation of off-resonance prepulses for clinical magnetization transfer contrast imaging at 0.2, 1.5, and 3.0 tesla. Invest Radiol 2008;43:16-26.
5. Kapila V, Wehrle CJ, Tuma F. Physiology, Spleen. In: StatPearls. Treasure Island (FL): StatPearls Publishing; May 1, 2023.
6. Sorokin EP, Basty N, Whitcher B, Liu Y, Bell JD, Cohen RL, Cule M, Thomas EL. Analysis of MRI-derived spleen iron in the UK Biobank identifies genetic variation linked to iron homeostasis and hemolysis. Am J Hum Genet 2022;109:1092-104.
7. Chandarana H, Do RK, Mussi TC, Jensen JH, Hajdu CH, Babb JS, Taouli B. The effect of liver iron deposition on hepatic apparent diffusion coefficient values in cirrhosis. AJR Am J Roentgenol 2012;199:803-8.
8. Xiao BH, Wáng YXJ. Different tissue types display different signal intensities on b = 0 images and the implications of this for intravoxel incoherent motion analysis: Examples from liver MRI. NMR Biomed 2021;34:e4522.
9. Lavdas I, Rockall AG, Castelli F, Sandhu RS, Papadaki A, Honeyfield L, Waldman AD, Aboagye EO. Apparent Diffusion Coefficient of Normal Abdominal Organs and Bone Marrow From Whole-Body DWI at 1.5 T: The Effect of Sex and Age. AJR Am J Roentgenol 2015;205:242-50.
10. DeMulder D, Ascher SM. Uterine Leiomyosarcoma: Can MRI Differentiate Leiomyosarcoma From Benign Leiomyoma Before Treatment? AJR Am J Roentgenol 2018;211:1405-15.
11. Bura V, Pintican RM, David RE, Addley HC, Smith J, Jimenez-Linan M, Lee J, Freeman S, Georgiu C. MRI findings in-between leiomyoma and leiomyosarcoma: a Rad-Path correlation of degenerated leiomyomas and variants. Br J Radiol 2021;94:20210283.
12. Barral M, Placé V, Dautry R, Bendavid S, Cornelis F, Foucher R, Guerrache Y, Soyer P. Magnetic resonance imaging features of uterine sarcoma and mimickers. Abdom Radiol (NY) 2017;42:1762-72.
13. Paudyal B, Paudyal P, Tsushima Y, Oriuchi N, Amanuma M, Miyazaki M, Taketomi-Takahashi A, Nakazato Y, Endo K. The role of the ADC value in the characterisation of renal carcinoma by diffusion-weighted MRI. Br J Radiol 2010;83:336-43.
14. Padhani AR, Liu G, Koh DM, Chenevert TL, Thoeny HC, Takahara T, Dzik-Jurasz A, Ross BD, Van Cauteren M, Collins D, Hammoud DA, Rustin GJ, Taouli B, Choyke PL. Diffusion-weighted magnetic resonance imaging as a cancer biomarker: consensus and recommendations. Neoplasia 2009;11:102-25.
15. Cao L, Chen J, Duan T, Wang M, Jiang H, Wei Y, Xia C, Zhou X, Yan X, Song B. Diffusion kurtosis imaging (DKI) of hepatocellular carcinoma: correlation with microvascular invasion and histologic grade. Quant Imaging Med Surg 2019;9:590-602.
16. Gandhi D, Sharma P, Garg G, Songmen S, Solanki S, Singh T. Intrahepatic splenosis demonstrated by diffusion weighted MRI with histologic confirmation. Radiol Case Rep 2020;15:602-6.
17. Nonomura Y, Yasumoto M, Yoshimura R, Haraguchi K, Ito S, Akashi T, Ohashi I. Relationship between bone

marrow cellularity and apparent diffusion coefficient. J Magn Reson Imaging 2001;13:757-60.
18. Li TQ, Chen ZG, Hindmarsh T. Diffusion-weighted MR imaging of acute cerebral ischemia. Acta Radiol 1998;39:460-73.
19. Knight RA, Dereski MO, Helpern JA, Ordidge RJ, Chopp M. Magnetic resonance imaging assessment of evolving focal cerebral ischemia. Comparison with histopathology in rats. Stroke 1994;25:1252-61; discussion 1261-2.
20. Wansapura JP, Holland SK, Dunn RS, Ball WS Jr. NMR relaxation times in the human brain at 3.0 tesla. J Magn Reson Imaging 1999;9:531-8.
21. Jerome NP, d'Arcy JA, Feiweier T, Koh DM, Leach MO, Collins DJ, Orton MR. Extended T2-IVIM model for correction of TE dependence of pseudo-diffusion volume fraction in clinical diffusion-weighted magnetic resonance imaging. Phys Med Biol 2016;61:N667-80.
22. Egnell L, Jerome NP, Andreassen MMS, Bathen TF, Goa PE. Effects of echo time on IVIM quantifications of locally advanced breast cancer in clinical diffusion-weighted MRI at 3 T. NMR Biomed 2022;35:e4654.

Cite this article as: Wáng YXJ, Zhao KX, Ma FZ, Xiao BH. The contribution of T2 relaxation time to MRI-derived apparent diffusion coefficient (ADC) quantification and its potential clinical implications. Quant Imaging Med Surg 2023;13(10):7410-7416. doi: 10.21037/qims-23-1106

